Human Molecular Genetics, 2008, Vol. 17, No. 2 **313–322**
doi:10.1093/hmg/ddm309
Advance Access published on October 22, 2007

CHMP2B C-truncating mutations in frontotemporal lobar degeneration are associated with an aberrant endosomal phenotype *in vitro*

Julie van der Zee[1,2,4], Hazel Urwin[6], Sebastiaan Engelborghs[3,4,5], Marc Bruyland[8], Rik Vandenberghe[9], Bart Dermaut[10], Tim De Pooter[1,2,4], Karin Peeters[1,2,4], Patrick Santens[10], Peter P. De Deyn[3,4,5], Elizabeth M. Fisher[7], John Collinge[6], Adrian M. Isaacs[6] and Christine Van Broeckhoven[1,2,4,*]

[1]Neurodegenerative Brain Diseases Group, Department of Molecular Genetics, VIB, [2]Laboratory of Neurogenetics, [3]Laboratory of Neurochemistry and Behavior, Institute Born-Bunge, [4]University of Antwerp, [5]Memory Clinic, Department of Neurology, ZNA Middelheim General Hospital, Antwerpen, Belgium, [6]MRC Prion Unit and [7]Department of Neurodegenerative Disease, Institute of Neurology, University College London, London, UK, [8]Department of Neurology, AZ Zusters van Barmhartigheid, Ronse, Belgium, [9]Department of Neurology, University Hospital Gasthuisberg, University of Leuven, Leuven, Belgium and [10]Department of Neurology, University Hospital Ghent, University of Ghent, Gent, Belgium

Received July 11, 2007; Revised and Accepted October 16, 2007

The charged multivesicular body protein 2B gene (*CHMP2B*) was recently associated with frontotemporal lobar degeneration (FTLD) linked to chromosome 3 in a Danish FTLD family (FTD-3). In this family, a mutation in the acceptor splice site of exon 6 produced two aberrant transcripts predicting two C-truncated CHMP2B proteins due to a read through of intron 5 (p.Met178ValfsX2) and a cryptic splicing event within exon 6 (p.Met178LeufsX30). Extensive mutation analysis of *CHMP2B* in Belgian patients (*N*=146) identified one non-sense mutation in exon 5 (c.493C>T) in a familial FTLD patient, predicting a C-truncated protein p.Gln165X analogous to the Danish mutant proteins. Overexpression of Belgian p.Gln165X in human neuroblastoma SK-N-SH cells showed the formation of large, aberrant endosomal structures that were highly similar to those observed for Danish p.Met178ValfsX2. Together, these data suggest that C-truncating mutations in *CHMP2B* might underlie the pathogenic mechanism in FTLD by disturbing endosome function. We also describe a missense mutation in exon 5 of *CHMP2B* (p.Asn143Ser) in a familial patient with cortical basal degeneration. However, the pathogenic character of this mutation remains elusive.

INTRODUCTION

Frontotemporal lobar degeneration (FTLD) represents a clinically and pathologically heterogeneous group of primary neurodegenerative dementias with predominant frontal and/or temporal lobe symptoms. It can present as frontotemporal dementia (FTD), which comprises the major group. In FTD patients, behaviour and personality changes are predominant. Other patients present primarily with language dysfunction, with behavioural changes occurring later in the disease course. This group can be further classified into progressive non-fluent aphasia (PNFA) where patients experience difficulties in language expression and semantic dementia (SD) which is characterized by problems in word comprehension and naming (1,2). In addition, signs of parkinsonism can develop during the course of the disease, and in some patients,

*To whom correspondence should be addressed at: Department of Molecular Genetics, Neurodegenerative Brain Diseases Group, VIB University of Antwerp—CDE, Universiteitsplein 1, BE-2610 Antwerpen, Belgium. Tel: +32 32651001; Fax: +32 32651012; Email: christine.vanbroeckhoven@ua.ac.be

FTLD concurs with motor neuron disease. Like FTLD, progressive supranuclear palsy (PSP) and corticobasal degeneration (CBD) are focal neurodegenerative disorders with frequent personality changes, speech disturbances and parkinsonism. Multiple studies have demonstrated that there exists a significant clinical and pathological overlap between FTLD, PSP and CBD. Patients presenting clinically as CBD or PSP have been described with FTLD with tau as well as ubiquitin positive pathology (3–5). Conversely, PSP and CBD pathologies can underlie clinical symptoms of FTLD (6–8). The degree of overlap between CBD, PSP and FTLD suggests that these relatively rare conditions might be part of a more common spectrum of neurodegenerative disorders.

The majority of FTLD families have been linked to chromosomes 17q21 and a wide range of mutations have been identified in the microtubule associated protein tau gene (*MAPT*) (9) and the progranulin gene (*PGRN*) (10,11) (AD&FTD Mutation database: http://www.molgen.ua.ac.be/FTDmutations). In a large Danish kindred, however, dominant FTLD was linked to the pericentromeric region of chromosome 3 (FTD-3) (12). Ten years later, a mutation was identified in the gene coding for the charged multivesicular body (MVB) protein 2B—also known as chromatin-modifying protein 2B—(*CHMP2B*) located at 3p11.2, that segregated with FTLD in this family (13).

CHMP2B encodes a component of the heteromeric ESCRT-III complex (Endosomal Sorting Complex Required for Transport III). In eukaryotic cells, the sorting of cell surface receptors for recycling to the plasma membrane or the Golgi complex, or for degradation by the lysosome is mediated by the MVB pathway (14). MVBs are late endosomal structures which fuse with the lysosome and are formed by invagination and budding of vesicles from the limiting membrane of endosomes into the endosomal lumen. This process requires the transient formation of three ESCRT complexes I–III (14,15). These multisubunit protein complexes are recruited from the cytoplasm and were first identified in yeast as class E Vps (vacuolar protein sorting) proteins. Deletion or loss of function of each of these proteins has been shown to induce accumulation of transmembrane proteins in large aberrant structures on the limiting membrane of enlarged dysmorphic endosomes, referred to as class E compartments (14,16). Yeast Vps proteins have one or more human orthologues, pointing to a greater complexity of the MVB pathway in mammals. CHMP2B is one of the two human orthologues of the yeast Vps2 protein and forms a component of the ESCRT-III complex. The six ESCRT-III proteins in yeast have at least 10 apparent human homologues called the charged MVB proteins or CHMP proteins (17). CHMP proteins cycle between a monomeric state in the cytosol and an oligomerized state in large ESCRT-III complexes on the limiting membrane of the endosome (14,18–20). ESCRT-III functions in the concentration of ubiquitinated endosomal cargo for invagination into the MVB intralumenal vesicles (14,18). After proteins are sorted, ESCRT-III recruits an AAA-ATPase (VPS4) for active dissociation of the membrane-bound complex and recycling of its components into the cytosol for further rounds of MVB sorting (14,18,21). CHMP proteins are conserved throughout eukaryotic evolution and show strong structural homology. They are small ~200–250 amino acid soluble coiled-coil proteins with characteristic basic N-terminal and acidic C-terminal halves (18). CHMP2B is a 213-amino-acid protein that contains, next to the two coiled-coil domains (residues 1–50 and 120–150), a large predicted Snf-7 domain (residues 16–178). It is expressed in all major regions of the brain and in all neuronal populations, especially in hippocampus, frontal and temporal lobes and cerebellum (13).

The Danish *CHMP2B* G-to-C mutation was found in the acceptor splice site of exon 6 and was shown to produce two abundant splice variants in brain predicting proteins with altered C-terminal sequences (13) (Fig. 1C). In the first transcript referred to as $CHMP2B^{Intron5}$, read-through of intron 5 caused a deletion of 36 amino acids creating a C-altered tail of one Val-residue (p.Met178ValfsX2). In the second mutant transcript $CHMP2B^{\Delta 10}$, the use of a cryptic splice site within exon 6 deleted 10 bp and produced a C-truncated protein with 29 residues of nonsense sequence (p.Met178LeufsX30). Further, overexpression of these mutant transcripts in rat PC12 cells caused an aberrant phenotype characterized by the accumulation of mutant CHMP2B on the outer membrane of enlarged, dysmorphic endosomes, similar to the observations made in yeast *Vps* mutants (13). In addition to the Danish splice site mutation, a missense mutation (p.Asp148Tyr) was reported in an SD patient without clear family history of neurodegenerative disease (13). However, altogether *CHMP2B* appeared to be a rare cause of FTLD since several large FTLD patient series failed to detect any *CHMP2B* mutations (22–24).

In the present study, we performed an extensive exonic mutation analysis of *CHMP2B* in a Belgian patient series comprising 134 unrelated FTLD patients. Considering the clinicopathological overlap between FTLD, CBD and PSP, we also included seven patients with a clinical diagnosis of CBD and five patients diagnosed with PSP. In a familial FTLD patient, we identified a novel nonsense mutation in exon 5 resulting in a stably expressed mutant transcript coding for a C-truncating protein (p.Gln165X). Overexpression studies showed a similar cellular effect for the Belgian and Danish C-truncated proteins with both leading to an aberrant endosomal phenotype. Further, we observed one missense mutation in exon 5 (p.Asn143Ser) in a familial CBD patient.

RESULTS

CHMP2B genetic studies

In a Belgian series of 146 patients who had previously been screened for mutations in the genes *MAPT*, *PGRN*, *PSEN1* and *VCP*, we identified two mutations located within *CHMP2B* exon 5. A C-to-T transition (c.493C>T; FTLD patient DR157.1) at 39 bp near the 3′ end of exon 5 (Fig. 1A and B), predicted a stop codon resulting in a C-truncated protein of 165 amino acids, p.Gln165X (Fig. 1C). RT–PCR analysis of *CHMP2B* complementary DNA (cDNA) of the patient's lymphoblasts confirmed the presence of mutant transcript (Fig. 1B). A second mutation A-to-G was identified near the 5′ end of exon 5 (c.428A>G; CBD patient DR70.1) (Fig. 1A and B), predicting an amino acid substitution, p.Asn143Ser. Asn143 is a highly conserved

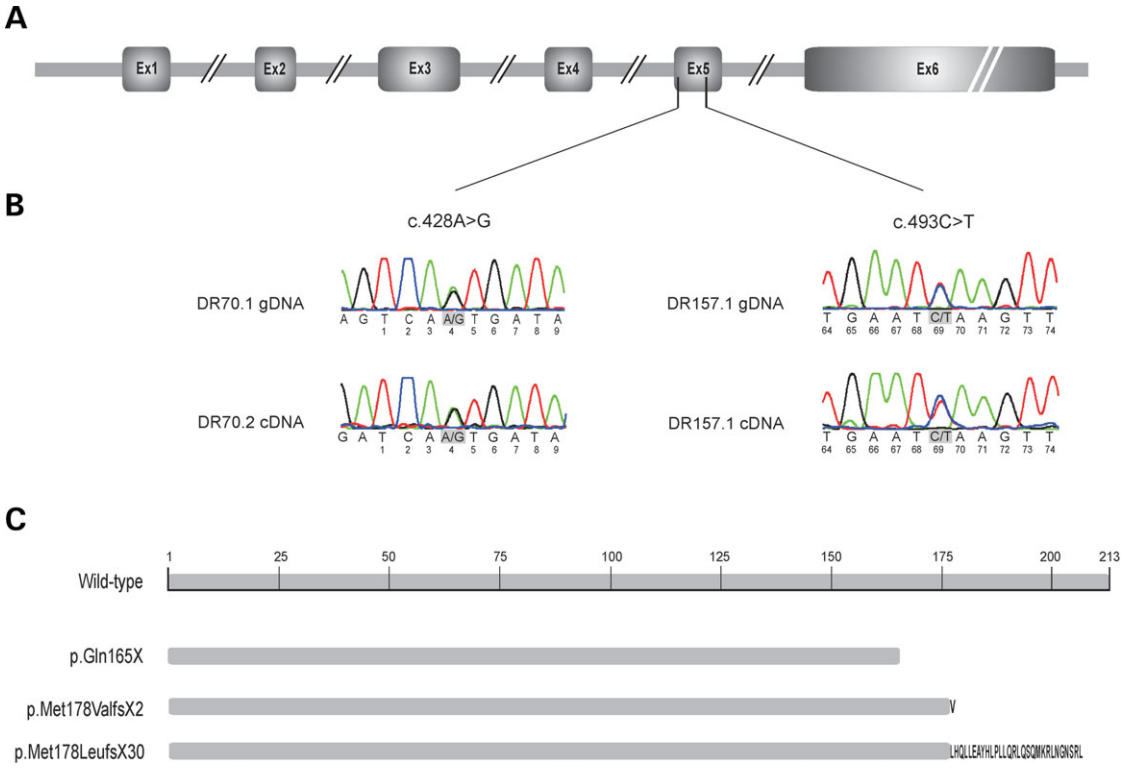

Figure 1. *CHMP2B* C-truncating mutations cause FTLD linked to chromosome 3. (**A**) Schematic representation of the *CHMP2B* gene. (**B**) Sequence traces of *CHMP2B* mutations identified in a Belgian FTLD patient (c.493C>T; DR157.1) and a CBD patient (c.428A>G; DR70.1) on gDNA and on cDNA prepared from lymphoblasts of patient DR157.1 and an asymptomatic at-risk individual DR70.2. Numbering under nucleotides indicates the relative position in exon 5. (**C**) Schematic representation of the CHMP2B wild-type protein and C-truncated proteins encoded by the Belgian nonsense mutation p.Gln165X and the Danish splice site mutations p.Met178ValfsX2 and p.Met178LeufsX30. For the Danish C-truncated transcripts, altered amino acid sequences are given.

amino acid residue from human to *Drosophila* and is located in the conserved Snf7 domain (residues 16–178) as well as in the second coiled-coil domain (residues 120–150) of CHMP2B. The mutation is located near the splice acceptor site of exon 5, however, sequencing of lymphoblast *CHMP2B* cDNA showed only the wild-type and missense transcripts excluding the formation of aberrantly spliced transcripts (Fig. 1B). Both exon 5 mutations, c.493C>T and c.428A>G, were absent in 459 Belgian control individuals.

In the FTLD family DR157, we examined the presence of the mutation in available family members and performed haplotype segregation using a set of nine microsatellite markers (Fig. 2). None of the four at-risk individuals carried the p.Gln165X mutation or the risk haplotype. Both sisters of the index patient, aged 81 and 61, were without symptoms of FTLD. In the CBD family DR70, only one healthy at-risk individual was available for testing. This person carried the p.Asn143Ser mutation but was still below the onset age of the index patient (pedigree not shown for reasons of confidentiality).

Clinical phenotypes

The index patient of the FTLD family DR157 who carried the p.Gln165X mutation showed first signs of the disease at the age of 58. Dysgraphia was the earliest symptom which progressively deteriorated. Her family complained that she often repeated the same thing. There also was loss of decorum with mild disinhibition. Two years after disease onset, neurological testing showed a light disorientation in space and time. There was severe dysgraphia with dysorthographia and grammatical errors. The patient confabulated. Mild dyslexia, dyspraxia and severe dyscalculia were observed; however, delayed recall was preserved. The patient scored 21/30 on mini mental state examination (MMSE). Computer-assisted tomography (CT) scan showed a mild frontal cortical atrophy. At the age of 64, the patient was clearly disoriented in space and time, her handwriting had become unreadable and the dyslexia had severely worsened. She exhibited logorrhoea and perseverated. Dyspraxia had increased, and delayed recall was now clearly impaired. Her MMSE score had dropped to 7/30. The CT scan revealed generalized cortical atrophy, somewhat more pronounced at the temporal medial gyrus both left and right. Her mother and maternal aunt suffered from dementia and died without autopsy (Fig. 2). According to family informants, the brother of her grandmother and his son were also affected, but medical records could not be obtained.

The index patient in family DR70 who carried the missense mutation p.Asn143Ser was diagnosed with CBD. Symptoms started ~2 years prior to clinical diagnosis at 73 years with progressive deterioration of memory, disorientation in space and time, behavioural problems, global aphasia with severe anomia and speech production problems, tendency to mutism, acalculia, dressing dyspraxia and important bradypsychisme. At diagnosis, she had an MMSE score of 11/30.

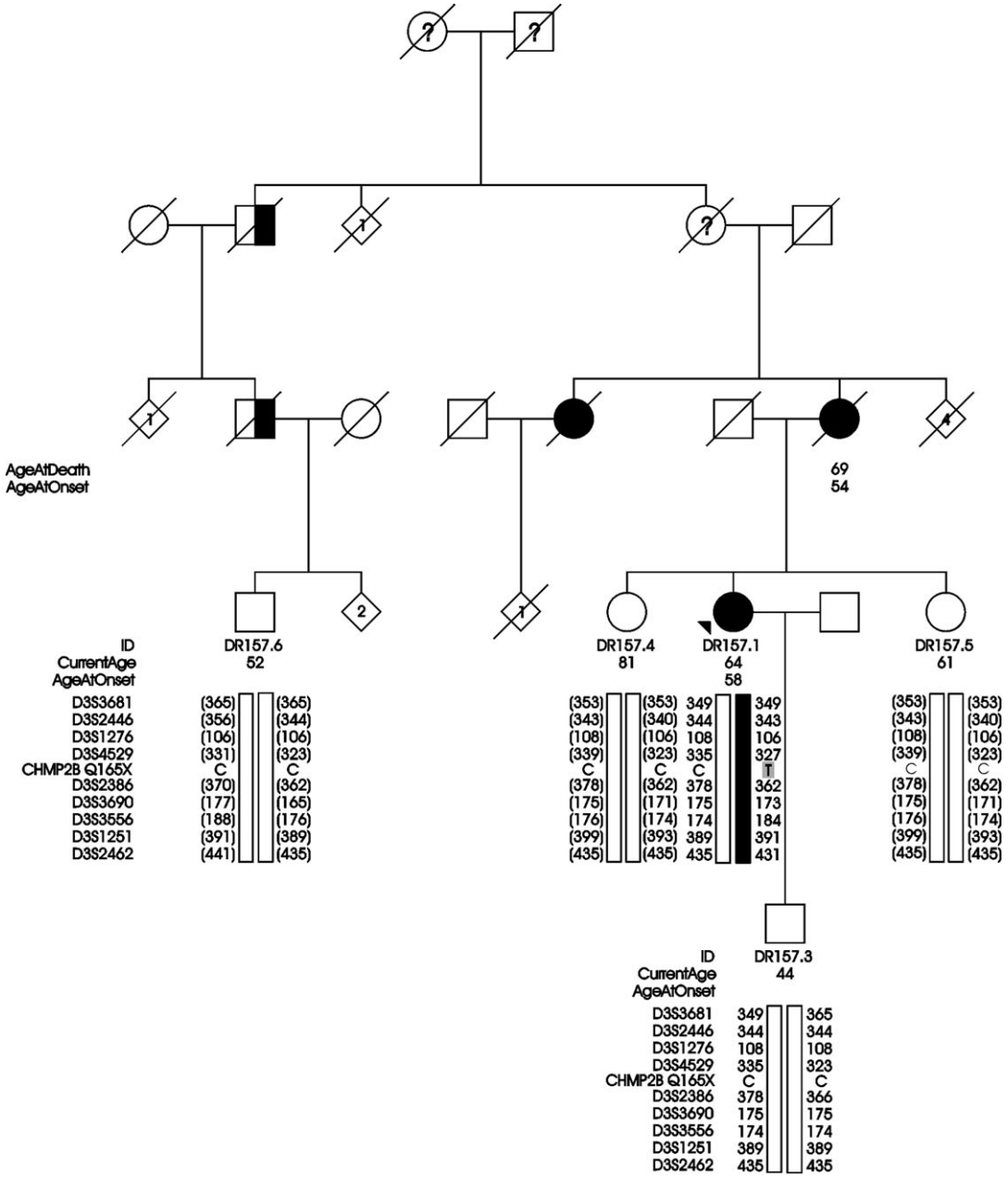

Figure 2. Pedigree of the Belgian FTLD family with the *CHMP2B* p.Gln165X mutation. Information on affection status, current age or age at death for deceased relatives and age at onset in patients are given when available. Open symbols represent unaffected individuals, filled symbols patients and half-filled symbols individuals who were affected according to family informants. An arrowhead identifies the index patient. The pedigree was anonymized to protect privacy of the family. The numbers within each diamond represent unaffected at-risk individuals. Segregation data are given for c.493C>T, p.Gln165X and nine flanking microsatellite markers. The black bar represents the risk haplotype. When the phase could not be determined, genotypes are given between parentheses.

Parallel with the cognitive decline, she developed an extrapyramidal syndrome presenting with resting tremor of the right foot and later in the disease course pronounced global rigidity and cogwheel phenomenon, hypomimia and hypokinesia, reduced arm swing and shuffling gait. Further, finger agnosia, vertical gaze palsy and vivid symmetrical tendon reflexes were reported. Structural imaging failed because the patient could not lie still. Single photon emission computed tomography (SPECT) scan showed diastasis of frontal cortical activity. The patient died at 80 years without autopsy. Genealogical investigation revealed a maternal aunt with dementia, whereas her mother died early at the age of 54.

Functional studies

We compared the subcellular localization of wild-type CHMP2B ($CHMP2B^{Wildtype}$), Belgian p.Gln165X ($CHMP2B^{Q165X}$), and the Danish p.Met178ValfsX2 ($CHMP2B^{Intron5}$) proteins in human neuroblastoma SK-N-SH cells that were transiently transfected with the respective N-terminal c-myc tagged expression

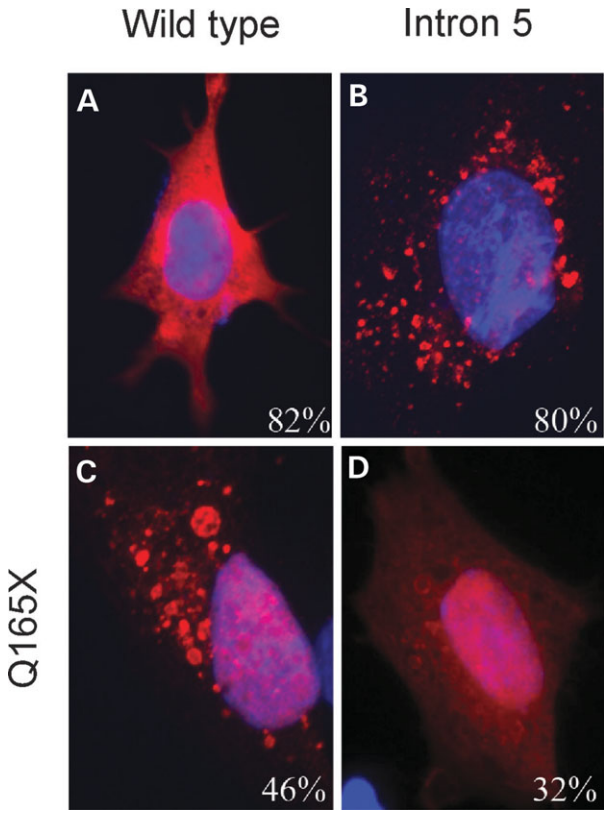

Figure 3. *CHMP2B* C-truncating mutations lead to aberrant endosomal structures. SK-N-SH cells transiently transfected with N-terminal c-myc-tagged expression constructs encoding recombinant proteins c-Myc-CHMP2B^{Wildtype}, c-Myc-CHMP2B^{Intron5} or c-Myc-CHMP2B^{Q165X}. Twenty-four hours post-transfection, cells were immunostained with anti-c-Myc antibody to visualize recombinant CHMP2B proteins. c-Myc staining is shown in red and DAPI staining in blue. (**A**) CHMP2B^{Wildtype} had predominantly diffuse staining. (**B**–**D**) Cells overexpressing CHMP2B^{Intron5} (B) or CHMP2B^{Q165X} (C and D) showed large aberrant vesicular structures. For CHMP2B^{Q165}, vesicular staining appeared on a background of nuclear and no cytoplasmic staining (46% of transfected cells) or with diffuse cytoplasmic and nuclear staining (32% of transfected cells).

constructs. Twenty-four hours post-transfection, localization of CHMP2B (visualized with an anti-c-myc antibody) showed large vesicular structures in the cells transfected with CHMP2B^{Intron5} (Fig. 3B) and CHMP2B^{Q165X} (Fig. 3C and D). This was in contrast to CHMP2B^{Wildtype} (Fig. 3A), which showed a generally diffuse pattern of staining. Occasional vesicular structures that were much smaller than those seen with the mutant constructs were observed, possibly due to the expected transient association of CHMP2B with endosomes. We also noted that many more cells per well expressed CHMP2B^{Wildtype} than the mutant constructs. This may be due to faster degradation or less efficient translation of the mutant proteins. This difference was confirmed by western blotting, which showed a greater level of CHMP2B^{Wildtype} than CHMP2B^{Intron5} and CHMP2B^{Q165X} in cell lysates from equivalent transfections (Supplementary Material, Fig. S1). CHMP2B^{Q165X} was also observed in the nucleus (Fig. 3C and D). This localization differed from CHMP2B^{Intron5} (Fig. 3B), which was generally excluded from the nucleus. These staining patterns were also observed at 48 h post-transfection as well as in a second cell line, SH-SY-5Y (Supplementary Material, Fig. S2). Blind counts of the localization of overexpressed CHMP2B proteins confirmed that the predominant cellular phenotype for CHMP2B^{Intron5} and CHMP2B^{Q165X} were large vesicular structures, whereas CHMP2B^{Wildtype} had predominantly diffuse staining. For CHMP2B^{Q165X}, the vesicular staining appeared either on a background of diffuse cytoplasmic and nuclear staining (32% of transfected cells) or more commonly with only nuclear and no cytoplasmic staining (46% of transfected cells) (Fig. 3C and D).

Immunostaining with the endosomal marker CD63 showed partial co-localization with CHMP2B-positive vesicular structures (Fig. 4), indicating that at least some of the vesicular structures are aberrant endosomal structures that may be analogous to the class E structures observed with ESCRT protein mutants in yeast (18). Co-localization was confirmed with a second late endosomal marker, LAMP-1 (data not shown).

DISCUSSION

To date, the Danish FTLD family (FTD-3) remains the only FTLD family linked to the pericentromeric region of chromosome 3 (13), complicating the identification of the underlying disease gene. Candidate gene sequencing identified a splice site mutation in *CHMP2B* segregating with the disease in the FTD-3 family, that produced two frameshift transcripts predicting the C-truncated proteins p.Met178ValfsX2 and p.Met178LeufsX30 (13), and excluded causal mutations in all other known genes in the candidate region (25). A potential pathogenic mechanism for the C-truncation of CHMP2B was suggested by the observation of an aberrant cellular endosomal phenotype upon overexpression of p.Met178ValfsX2 in PC12 cells (13). However, numerous mutation screening studies in series of sporadic and familial FTLD patients failed to identify additional pathogenic *CHMP2B* mutations (22–24), indicating that, if *CHMP2B* is the chromosome 3 gene, its genetic contribution to FTLD has to be very low.

In a Belgian patient series (N=146), we identified a novel nonsense mutation in a familial FTLD patient located in penultimate exon 5 of *CHMP2B*. The index patient developed the first signs of FTLD at the age of 58 and had a family history of dementia indicative of an autosomal dominant mode of inheritance. Only four healthy at-risk individuals (age range 44–81 years) were available for genetic studies, and segregation analysis revealed neither the mutation nor the risk haplotype. Notably, the oldest sister died without signs of disease at the age of 81, more than 20 years later than the disease onset in the proband. Unfortunately, no pathology data were yet available to support the clinical diagnosis of FTLD in this family since the index patient is still alive, and patients from previous generations died without autopsy.

Consistent with the Danish *CHMP2B* frameshift mutations (p.Met178ValfsX2 and p.Met178LeufsX30), the Belgian nonsense mutation predicted the formation of a C-truncated protein p.Gln165X lacking 49 amino acids (Fig. 1C). Sequencing of *CHMP2B* cDNA, derived by RT–PCR amplification of mRNA extracted from lymphoblasts of the index patient, confirmed the presence of the mutant transcript at apparently equal amounts as the wild-type transcript. The latter indicated

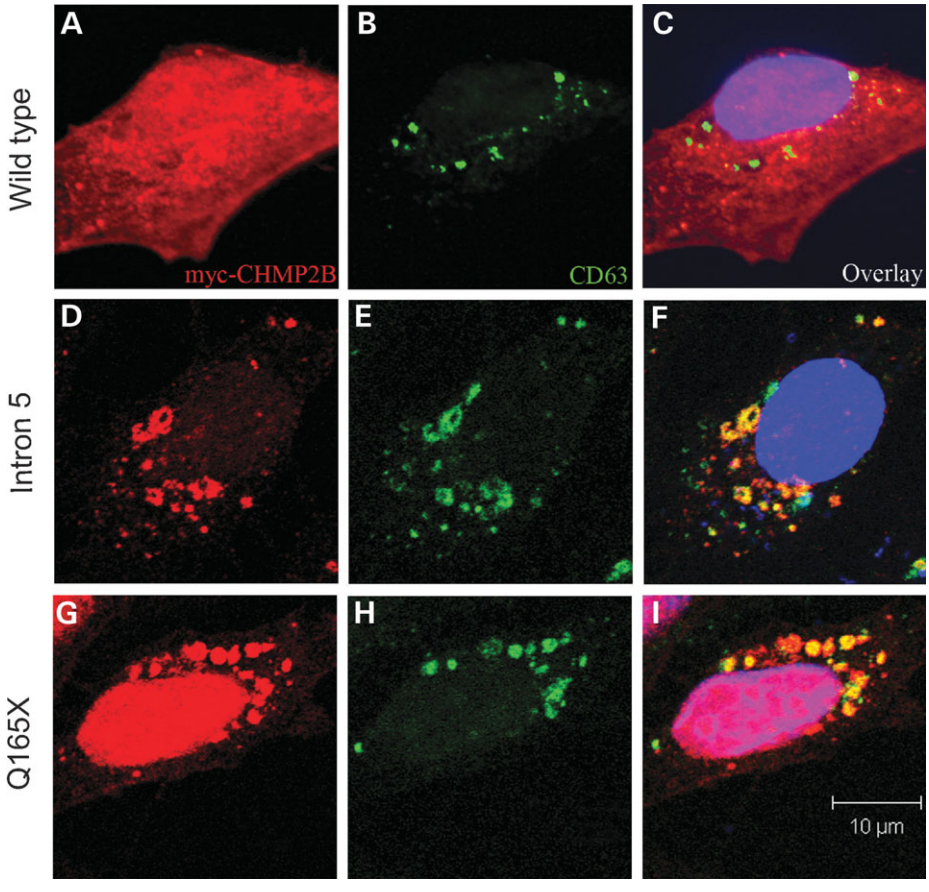

Figure 4. Aberrant endosomal structures caused by *CHMP2B* C-truncating mutants co-localize with late endosomal marker. Twenty-four hours post-transfection, SK-N-SH cells were double-stained with anti-c-Myc antibody in red (**A**, **D** and **G**) and anti-CD63 antibody in green (**B**, **E** and **H**). DAPI stain in blue. The images were merged to asses co-localization (**C**, **F** and **I**). CD63 showed partial co-localization with the CHMP2B positive vesicular structures.

that the mutant transcript escaped nonsense-mediated decay (NMD) and that C-truncated protein is likely to be formed. NMD is an mRNA surveillance system that degrades transcripts containing premature stop codons to prevent the formation of aberrant truncated proteins. For stop codons in the penultimate exon of a gene (exon 5 for *CHMP2B*), NMD generally only occurs when the mutation is located at a distance greater than ~55 bp from the final exon junction (26). The Belgian *CHMP2B* nonsense mutation is located at 39 bp from the exons 5–6 junction (Fig. 1), and as expected escapes NMD.

Here we showed that overexpression of Belgian $CHMP2B^{Q165X}$ in human neuroblastoma cells leads to accumulation of mutant protein on enlarged vesicular structures in a similar distribution as Danish $CHMP2B^{Intron5}$. Initially, we reported enlarged vesicular structures in $CHMP2B^{Intron5}$ expressing PC12 cells (13), and this phenotype was very recently observed in mouse cortical neurons overexpressing $CHMP2B^{Intron5}$ (27). The enlarged vesicles partially co-localized with the late endosomal marker CD63, consistent with the role of CHMP2B and the ESCRT-III complex in endosomal function. C-terminal truncation of CHMP2B disrupts its strong charge distribution. Previous studies showed that the acidic C-terminus of CHMP proteins functions as auto-inhibitory domain through intramolecular interactions with their basic N-terminal halves, thereby closing the protein and hiding the membrane binding and polymerization properties of the N-terminal half (19,20,28,29). Normally, CHMP proteins shuttle between this default, closed inactive soluble state in the cytosol and an open activated state, which permits them to polymerize into heteromeric ESCRT-III complexes on the endosomal membrane. However, C-terminal truncation relieves the inhibitory effect of the C-terminus, thereby forcing the proteins into a constitutively active state. This causes the truncated proteins to remain bound in ESCRT-III complexes that accumulate on the endosomal membrane. Moreover, CHMP proteins interact with the VPS4 AAA-ATPase through sequences on their C-terminus (19,30). As such, C-terminal truncation would prevent binding with VPS4, which is mandatory for active dissociation of the complex. Therefore, C-terminal truncation of CHMP2B would be predicted to block MVB formation as the mutant, constitutively active proteins can no longer dissociate, thereby preventing the invagination process and intraluminal vesicle formation. In support of this hypothesis, there is evidence that C-terminal truncations of ESCRT-III proteins can functionally affect endosomal pathways. Two independent studies have shown that C-terminal truncations in CHMP2A (19), CHMP2B (20) and other CHMP proteins (19,20) inhibited virus budding, a process for which the ESCRT complexes are required.

Together, these findings suggest that CHMP2B pathogenesis results from the production of C-truncated proteins that in turn impair endosomal functioning. However, this is in

contrast to the recent finding of a *CHMP2B* C-truncating mutation p.Arg186X in two apparently healthy at-risk individuals from an Afrikaner FTLD family (24). The mutation was excluded in their affected father, as well as in five of his diseased relatives. Segregation analysis indicated that the two unaffected children had inherited p.Arg186X from their mother who had died at the age of 69 without signs of memory or neurological impairments. The Afrikaner C-truncation is smaller than that in $CHMP2B^{Intron5}$ and $CHMP2B^{Q165X}$, but preliminary functional analysis showed that overexpression of this truncated protein also leads to an enlarged endosomal phenotype (Supplementary Material, Fig. S3).

These contradictory data call for cautious interpretation of the current genetic and *in vitro* functional data. If our data are correct and C-truncated *CHMP2B* mutations are pathogenic by impairing endosomal functioning, we would have to assume that in the Afrikaner family the mother died before onset of disease and that both middle-aged mutation carriers might still develop the disease at a later age. This is not impossible given that FTLD is characterized by a very wide onset range, also within families, pointing to onset-modifying factors (2). Alternatively, our functional data are misleading due to an overinterpretation of the cellular phenotype which is produced by non-physiological overexpression of the C-truncated proteins, despite the evidence described above that C-terminal truncations can have inhibitory effects on ESCRT protein functions (19,20). Possibly a more specific cellular assay will distinguish between the Afrikaner and the Danish and Belgian mutations. Finally, since in the Belgian FTLD family, we still lack conclusive segregation data linking the *CHMP2B* nonsense mutation to the disease, we cannot rule out that *CHMP2B* is not the FTD-3 gene and that the aberrant cellular phenotype is unrelated to FTLD. However, the absence of mutations in any of the other known genes located in the FTD-3 locus (25) supports the notion that *CHMP2B* is the causative gene, unless the disease mutation resides in an as yet uncharacterized gene in the FTD-3 candidate region. Also, a mutation in a regulatory region or a copy number variation remains possible, as these types of mutations would not have been detected by the screening methods used.

The second mutation we observed was a missense mutation, p.Asn143Ser, in a patient with clinical diagnosis of CBD and first symptoms around the age of 73. At least one other relative was reportedly demented. The p.Asn143Ser mutation was transmitted to an at-risk individual; however, this person's age was far below the onset age of the index patient. Also in this family, we had no autopsy data available nor did we have samples of patients in previous generations. p.Asn143Ser changes a highly conserved residue located in the Snf7 domain (residues 16–178) as well as the C-terminal coiled-coil domain (residues 120–150) of the protein. Protein–protein interaction studies in yeast have shown that Vps4 binds to ESCRT-III through coiled-coil interactions with the Vps2–Vps24 subcomplex (18). Hence, p.Asn143Ser could perturb normal coiled-coil interactions with Vps4 or another protein of the complex. Moreover, p.Asn143Ser was absent in 918 control chromosomes (minor allele frequency $<0.1\%$) adding to the evidence in favour of a pathogenic nature for this missense mutation. The previously identified p.Asp148Tyr (13) affects the same conserved domains. In addition, the acidic Asp-residue is substituted by a hydrophobic residue, which could in turn affect the charge distribution of the protein. Overexpression of the missense mutant p.Asp148Tyr did not lead to an enlarged endosomal phenotype (Urwin and Isaacs, unpublished data), suggesting that the missense mutations, if pathogenic, may have a more subtle cellular phenotype. It is certainly plausible that endosome function could be impaired without formation of large aberrant endosomes. This would be consistent with a recent study that identified missense mutations in *CHMP4B* in families with autosomal dominant cataracts (31). Overexpression of the missense mutations did not give a cellular phenotype, whereas a truncated form of CHMP4B did lead to enlarged endosomes, and expressing the missense mutations within a truncated CHMP4B protein led to a more severe phenotype.

In conclusion, we identified another potential pathogenic mutation in *CHMP2B* in a familial FTLD patient. Of interest is that this nonsense mutation, as the original Danish *CHMP2B* mutations, leads to a C-truncated protein because it occurs in the 3′ end of the penultimate exon 5 and therefore escapes NMD. Both the Danish and Belgian C-truncated mutations affect endosomal functioning in an *in vitro* overexpression cellular assay, supportive for a role for *CHMP2B* in the neurodegenerative process of FTLD. However, we should remain cautious in our interpretation of the genetic and functional data as long as we have not been able to translate the *in vitro* data to human or to an *in vivo* model such as transgenic mice. Nevertheless, it remains intriguing that the few *CHMP2B* nonsense and frameshift mutations producing premature stop codons are all found in the 3′ part of the gene and escape NMD leading to stable transcripts coding for potential pathogenic C-truncating CHMP2B proteins. This could argue against a chance finding of these mutations in familial FTLD patients since several examples are known of such mutations leading to neurological diseases or to a different clinical outcome (32).

Further, we showed that *CHMP2B* mutations could be involved in a broader spectrum of neurodegenerative disease including CBD. To date, a significant fraction of familial FTLD cannot yet be explained by mutations in the currently known FTLD genes, indicating that other genetic factors must be involved in the aetiology of this disease. Considering the molecular pathology of CHMP2B in FTLD, and the similar phenotypes that are observed *in vitro* with other members of the CHMP family, *CHMP* genes in general might be good functional candidate genes for FTLD as well as other neurodegenerative disorders.

MATERIALS AND METHODS

Patients and control individuals

Patients included in this study were derived from a prospective Belgian study of neurodegenerative and vascular dementia (33) and from a collection of demented patients referred to our Molecular Diagnostic Unit for genetic testing. Patients were diagnosed using a standard protocol including

Table 1. Descriptives of Belgian patients and control individuals

	Individuals	Mean AAO/ AAI ± STDV (range)	Positive family history (%)	Male/ female
FTLD patients	134	63.51 ± 9.23 (40–90)	54 (40%)	71/63
FTLD unspecified	46			
FTLD, FTD	63			
FTLD, PNFA	9			
FTLD, SD	2			
FTD-ALS	9			
FTDP	5			
CBD patients	7	65.00 ± 9.92 (48–73)	3 (43%)	1/6
PSP patients	5	69.00 ± 4.53 (62–73)	1 (20%)	2/3
Control individuals	459	58.6 ± 16.0 (19–92)	—	207/253

AAO, age at onset in years is given for patients, AAI, age at inclusion in years for control individuals; STDV, standard deviation; FTLD, frontotemporal lobar degeneration; FTD, frontotemporal dementia; FTD-ALS, FTD with amyotrophic lateral sclerosis; FTDP, FTD with parkinsonism. A positive family history was defined as having at least one first-degree relative with dementia.

neurological examination, biochemical analyses, psychological evaluation using the MMSE test, and neuroimaging using CT and/or SPECT scan. Clinical diagnoses were based on established clinical criteria (1,33–35).

Patients and relatives were contacted by research nurses who gathered information on family history of dementia. Relatives of the index patient were asked to participate in a genetic study. Four hundred and fifty-nine neurologically healthy Belgian control individuals were analysed for identified *CHMP2B* mutations. All participants gave written informed consent. The research protocols for this study were approved by the Medical Ethical Committees of the Middelheim General Hospital and the University of Antwerp. Descriptives of the Belgian patients and control individuals are summarized in Table 1.

Sequencing analysis

CHMP2B mutation analysis was performed in 146 patients. Blood samples were collected for DNA extraction and the establishment of lymphoblast cell lines according to standard procedures. All *CHMP2B* exons and flanking intronic regions were PCR amplified on genomic DNA (20 ng). Amplification products were purified with 1 U antarctic phosphatase (New England Biolabs, Ipswich, MA, USA) and 1 U exonuclease I (New England Biolabs) and sequenced in both directions using the BigDye Terminator Cycle Sequencing kit v3.1 (Applied Biosystems, Foster City, CA, USA) on an ABI3730 automated sequencer (Applied Biosystems). Sequences were analysed using the Software Package NovoSNP (36). In patients, DR70.1 and DR157.1, carrying a *CHMP2B* mutation, mutations in other FTLD related genes—*MAPT*, *PGRN*, *PSEN1* and *VCP*—had previously been excluded (11,37,38).

Mutations observed in index patients were analysed in available DNA samples of relatives from DR157.1 and DR70.1 and were excluded in control individuals by pyrosequencing. PCR amplification was performed as mentioned above. Sequencing reactions were performed on a PSQ™ HS 96A Pyrosequenser (Biotage, Uppsala, Sweden, http://www.biotage.com/). PCR and sequencing primers are listed in Supplementary Material, Table S1.

Segregation analysis

Haplotype segregation analysis was performed in family DR157. In addition to the index patient, DNA samples of four at-risk individuals were obtained. Nine microsatellite markers in the proximity of *CHMP2B* were genotyped in the five family members. Genomic DNA (20 ng) was PCR amplified in three multiplex reactions. Fluorescently labelled products were resolved on an ABI3730 automated sequencer (Applied Biosystems). Genotypes were assigned using in-house developed genotyping software.

Transcript analysis

To test whether mutant *CHMP2B* transcripts were expressed, RT-PCR analysis on mRNA isolated from Epstein–Barr virus-transformed lymphoblasts of patient DR157.1 carrying c.493C>T and of an asymptomatic at-risk individual in family DR70, carrying c.428A>G. Total RNA was isolated using the RiboPure™ Kit (Ambion, Applied Biosystems Business, Austin, TX, USA). First-strand cDNA was synthesized starting from total RNA with random hexamer primers using the SuperScript III First-Strand Synthesis System for RT–PCR kit (Invitrogen, Carlsbad, CA, USA). cDNA primers were positioned in exons 3 and 6. RT–PCR products were analysed on a 2% agarose gel and sequenced. Primer sequences are listed in Supplementary Material, Table S1.

Overexpression of CHMP2B in SK-N-SH cells

The c-myc-tagged p.Gln165X expression construct was generated using the QuikChange Site Directed Mutagenesis kit (Stratagene) to introduce a stop codon at the appropriate position into our c-myc-tagged $CHMP2B^{Wildtype}$ construct that has been previously described (13). The change was confirmed by sequencing. All expression constructs were in the pLNCX2 mammalian expression vector (Clontech). SK-N-SH cells were maintained in DMEM (Sigma-Aldrich) supplemented with 10% heat inactivated fetal bovine serum (Invitrogen), glutamine and sodium pyruvate. Transfections were performed with Lipofecatime 2000 (Invitrogen). Anti-c-Myc antibody (Abcam, catalogue number ab9106) was used at 1:800 for immunofluorescence and anti-CD63 (University of Iowa Developmental Hybridoma Bank, catalogue number H5C6) was used at 1:400. Cell counts were performed by an investigator blind to the treatment condition. A minimum of 100 cells were counted for each expression construct and the average taken of three independent experiments. Images were obtained using either an Axioplan 2 MOT fluorescence microscope (Zeiss) or an LSM510 META confocal microscope (Zeiss).

SUPPLEMENTARY MATERIAL

Supplementary Material is available at HMG Online.

ACKNOWLEDGEMENTS

The authors are grateful to the patients and family members for their kind cooperation in this study, to the personnel of the VIB Genetic Service Facility (http://www.vibgeneticservicefacility.be) and of the Antwerp Biobank of the Institute Born-Bunge (IBB). J.v.d.Z. is a holder of a PhD fellowship of the IWT-F. The FWO-F provided a postdoctoral fellowship to S.E.

Conflict of Interest statement. None declared.

FUNDING

The research described in this paper was partly supported by the InterUniversity Attraction Poles (IAP) program P6/43 of the Belgian Federal Science Policy Office (BELSPO), the Fund for Scientific Research—Flanders (FWO-F), the Institute for the Promotion of Innovation through Science and Technology in Flanders (IWT-F), the Medical Research Foundation Antwerp and Neurosearch Antwerp and the Special Research Fund (BOF) of the University of Antwerp. A.M.I., H.U. and J.C. were funded by the UK Medical Research Council.

REFERENCES

1. Neary, D., Snowden, J.S., Gustafson, L., Passant, U., Stuss, D., Black, S., Freedman, M., Kertesz, A., Robert, P.H., Albert, M. *et al.* (1998) Frontotemporal lobar degeneration - A consensus on clinical diagnostic criteria. *Neurology*, **51**, 1546–1554.
2. Neary, D., Snowden, J. and Mann, D. (2005) Frontotemporal dementia. *Lancet Neurol.*, **4**, 771–780.
3. Boeve, B.F., Maraganore, D.M., Parisi, J.E., Ahlskog, J.E., Graff-Radford, N., Caselli, R.J., Dickson, D.W., Kokmen, E. and Petersen, R.C. (1999) Pathologic heterogeneity in clinically diagnosed corticobasal degeneration. *Neurology*, **53**, 795–800.
4. Grimes, D.A., Bergeron, C.B. and Lang, A.E. (1999) Motor neuron disease-inclusion dementia presenting as cortical-basal ganglionic degeneration. *Mov. Disord.*, **14**, 674–680.
5. Paviour, D.C., Lees, A.J., Josephs, K.A., Ozawa, T., Ganguly, M., Strand, C., Godbolt, A., Howard, R.S., Revesz, T. and Holton, J.L. (2004) Frontotemporal lobar degeneration with ubiquitin-only-immunoreactive neuronal changes: broadening the clinical picture to include progressive supranuclear palsy. *Brain*, **127**, 2441–2451.
6. Forman, M.S., Farmer, J., Johnson, J.K., Clark, C.M., Arnold, S.E., Coslett, H.B., Chatterjee, A., Hurtig, H.I., Karlawish, J.H., Rosen, H.J. *et al.* (2006) Frontotemporal dementia: Clinicopathological correlations. *Ann. Neurol.*, **59**, 952–962.
7. Josephs, K.A., Petersen, R.C., Knopman, D.S., Boeve, B.F., Whitwell, J.L., Duffy, J.R., Parisi, J.E. and Dickson, D.W. (2006) Clinicopathologic analysis of frontotemporal and corticobasal degenerations and PSP. *Neurology*, **66**, 41–48.
8. Kertesz, A., McMonagle, P., Blair, M., Davidson, W. and Munoz, D.G. (2005) The evolution and pathology of frontotemporal dementia. *Brain*, **128**, 1996–2005.
9. Hutton, M., Lendon, C.L., Rizzu, P., Baker, M., Froelich, S., Houlden, H., Pickering-Brown, S., Chakraverty, S., Isaacs, A., Grover, A. *et al.* (1998) Association of missense and 5′-splice-site mutations in tau with the inherited dementia FTDP-17. *Nature*, **393**, 702–705.
10. Baker, M., Mackenzie, I.R., Pickering-Brown, S.M., Gass, J., Rademakers, R., Lindholm, C., Snowden, J., Adamson, J., Sadovnick, A.D., Rollinson, S. *et al.* (2006) Mutations in progranulin cause tau-negative frontotemporal dementia linked to chromosome 17. *Nature*, **442**, 916–919.
11. Cruts, M., Gijselinck, I., van der Zee, J., Engelborghs, S., Wils, H., Pirici, D., Rademakers, R., Vandenberghe, R., Dermaut, B., Martin, J.J. *et al.* (2006) Null mutations in progranulin cause ubiquitin-positive frontotemporal dementia linked to chromosome 17q21. *Nature*, **442**, 920–924.
12. Brown, J., Ashworth, A., Gydesen, S., Sorensen, A., Rossor, M., Hardy, J. and Collinge, J. (1995) Familial non-specific dementia maps to chromosome 3. *Hum. Mol. Genet.*, **4**, 1625–1628.
13. Skibinski, G., Parkinson, N.J., Brown, J.M., Chakrabarti, L., Lloyd, S.L., Hummerich, H., Nielsen, J.E., Hodges, J.R., Spillantini, M.G., Thusgaard, T. *et al.* (2005) Mutations in the endosomal ESCRTIII-complex subunit CHMP2B in frontotemporal dementia. *Nat. Genet.*, **37**, 806–808.
14. Babst, M. (2005) A protein's final ESCRT. *Traffic.*, **6**, 2–9.
15. Babst, M., Katzmann, D.J., Snyder, W.B., Wendland, B. and Emr, S.D. (2002) Endosome-associated complex, ESCRT-II, recruits transport machinery for protein sorting at the multivesicular body. *Dev. Cell*, **3**, 283–289.
16. Rieder, S.E., Banta, L.M., Kohrer, K., McCaffery, J.M. and Emr, S.D. (1996) Multilamellar endosome-like compartment accumulates in the yeast vps28 vacuolar protein sorting mutant. *Mol. Biol. Cell*, **7**, 985–999.
17. von Schwedler, U.K., Stuchell, M., Muller, B., Ward, D.M., Chung, H.Y., Morita, E., Wang, H.E., Davis, T., He, G.P., Cimbora, D.M. *et al.* (2003) The protein network of HIV budding. *Cell*, **114**, 701–713.
18. Babst, M., Katzmann, D.J., Estepa-Sabal, E.J., Meerloo, T. and Emr, S.D. (2002) ESCRT-III: An endosome-associated heterooligomeric protein complex required for MVB sorting. *Dev. Cell*, **3**, 271–282.
19. Shim, S., Kimpler, L.A. and Hanson, P.I. (2007) Structure/function analysis of four core ESCRT-III proteins reveals common regulatory role for extreme C-terminal domain. *Traffic.*, **8**, 1068–1079.
20. Zamborlini, A., Usami, Y., Radoshitzky, S.R., Popova, E., Palu, G. and Gottlinger, H. (2006) Release of autoinhibition converts ESCRT-III components into potent inhibitors of HIV-1 budding. *Proc. Natl Acad. Sci. USA*, **103**, 19140–19145.
21. Babst, M., Wendland, B., Estepa, E.J. and Emr, S.D. (1998) The Vps4p AAA ATPase regulates membrane association of a Vps protein complex required for normal endosome function. *EMBO J.*, **17**, 2982–2993.
22. Cannon, A., Baker, M., Boeve, B., Josephs, K., Knopman, D., Petersen, R., Parisi, J., Dickison, D., Adamson, J., Snowden, J. *et al.* (2006) CHMP2B mutations are not a common cause of frontotemporal lobar degeneration. *Neurosci. Lett.*, **398**, 83–84.
23. Rizzu, P., van Mil, S.E., Anar, B., Rosso, S.M., Kaat, L.D., Heutink, P. and Van Swieten, J.C. (2006) CHMP2B mutations are not a cause of dementia in Dutch patients with familial and sporadic frontotemporal dementia. *Am. J. Med. Genet. B Neuropsychiatr. Genet*, **141**, 944–946.
24. Momeni, P., Rogaeva, E., Van Deerlin, V., Yuan, W., Grafman, J., Tierney, M., Huey, E., Bell, J., Morris, C.M., Kalaria, R.N. *et al.* (2006) Genetic variability in CHMP2B and frontotemporal dementia. *Neurodegener. Dis.*, **3**, 129–133.
25. Momeni, P., Bell, J., Duckworth, J., Hutton, M., Mann, D., Brown, S.P. and Hardy, J. (2006) Sequence analysis of all identified open reading frames on the frontal temporal dementia haplotype on chromosome 3 fails to identify unique coding variants except in CHMP2B. *Neurosci. Lett.*, **410**, 77–79.
26. Inoue, K., Khajavi, M., Ohyama, T., Hirabayashi, S., Wilson, J., Reggin, J.D., Mancias, P., Butler, I.J., Wilkinson, M.F., Wegner, M. *et al.* (2004) Molecular mechanism for distinct neurological phenotypes conveyed by allelic truncating mutations. *Nat. Genet.*, **36**, 361–369.
27. Lee, J.A., Beigneux, A., Ahmad, S.T., Young, S.G. and Gao, F.B. (2007) ESCRT-III dysfunction causes autophagosome accumulation and neurodegeneration. *Curr. Biol*, **17**, 1561–1567.
28. Whitley, P., Reaves, B.J., Hashimoto, M., Riley, A.M., Potter, B.V. and Holman, G.D. (2003) Identification of mammalian Vps24p as an effector of phosphatidylinositol 3,5-bisphosphate-dependent endosome compartmentalization. *J. Biol. Chem.*, **278**, 38786–38795.
29. Lin, Y., Kimpler, L.A., Naismith, T.V., Lauer, J.M. and Hanson, P.I. (2005) Interaction of the mammalian endosomal sorting complex required for transport (ESCRT) III protein hSnf7-1 with itself, membranes, and the AAA+ ATPase SKD1. *J. Biol. Chem.*, **280**, 12799–12809.
30. Scott, A., Gaspar, J., Stuchell-Brereton, M.D., Alam, S.L., Skalicky, J.J. and Sundquist, W.I. (2005) Structure and ESCRT-III protein interactions of the MIT domain of human VPS4A. *Proc. Natl Acad. Sci. USA*, **102**, 13813–13818.

31. Shiels, A., Bennett, T.M., Knopf, H.L., Yamada, K., Yoshiura, K., Niikawa, N., Shim, S. and Hanson, P.I. (2007) CHMP4B, a novel gene for autosomal dominant cataracts linked to chromosome 20q. *Am. J. Hum. Genet.*, **81**, 596–606.
32. Khajavi, M., Inoue, K. and Lupski, J.R. (2006) Nonsense-mediated mRNA decay modulates clinical outcome of genetic disease. *Eur. J. Hum. Genet.*, **14**, 1074–1081.
33. Engelborghs, S., Dermaut, B., Goeman, J., Saerens, J., Marien, P., Pickut, B.A., Van den Broeck, M., Serneels, S., Cruts, M., Van Broeckhoven, C. *et al.* (2003) Prospective Belgian study of neurodegenerative and vascular dementia: APOE genotype effects. *J. Neurol. Neurosurg. Psychiatry*, **74**, 1148–1151.
34. Litvan, I., Agid, Y., Calne, D., Campbell, G., Dubois, B., Duvoisin, R.C., Goetz, C.G., Golbe, L.I., Grafman, J., Growdon, J.H. *et al.* (1996) Clinical research criteria for the diagnosis of progressive supranuclear palsy (Steele–Richardson–Olszewski syndrome): report of the NINDS-SPSP International Workshop. *Neurology*, **47**, 1–9.
35. Litvan, I., Agid, Y., Goetz, C., Jankovic, J., Wenning, G.K., Brandel, J.P., Lai, E.C., Verny, M., Ray-Chaudhuri, K., McKee, A. *et al.* (1997) Accuracy of the clinical diagnosis of corticobasal degeneration: a clinicopathologic study. *Neurology*, **48**, 119–125.
36. Weckx, S., Del Favero, J., Rademakers, R., Claes, L., Cruts, M., De Jonghe, P., Van Broeckhoven, C. and De Rijk, P. (2005) novoSNP, a novel computational tool for sequence variation discovery. *Genome Res.*, **15**, 436–442.
37. van der Zee, J., Gijselinck, I., Pirici, D., Kumar-Singh, S., Cruts, M. and Van Broeckhoven, C. (2007) Frontotemporal lobar degeneration with ubiquitin-positive inclusions: a molecular genetic update. *Neurodegener. Dis.*, **4**, 227–235.
38. van der Zee, J., Le Ber, I., Maurer-Stroh, S., Engelborghs, S., Gijselinck, I., Camuzat, A., Brouwers, N., Vandenberghe, R., Sleegers, K., Hannequin, D. *et al.* (2007) Mutations other than null mutations producing a pathogenic loss of progranulin in frontotemporal dementia. *Hum. Mutat.*, **28**, 416.